# Dalton Transactions

## Accepted Manuscript

This article can be cited before page numbers have been issued, to do this please use: Y. Borguet, G. Zaragoza, A. Demonceau and L. Delaude, *Dalton Trans.*, 2015, DOI: 10.1039/C5DT00433K.


This is an *Accepted Manuscript*, which has been through the Royal Society of Chemistry peer review process and has been accepted for publication.

*Accepted Manuscripts* are published online shortly after acceptance, before technical editing, formatting and proof reading. Using this free service, authors can make their results available to the community, in citable form, before we publish the edited article. We will replace this *Accepted Manuscript* with the edited and formatted *Advance Article* as soon as it is available.

You can find more information about *Accepted Manuscripts* in the Information for Authors.

Please note that technical editing may introduce minor changes to the text and/or graphics, which may alter content. The journal's standard Terms & Conditions and the Ethical guidelines still apply. In no event shall the Royal Society of Chemistry be held responsible for any errors or omissions in this *Accepted Manuscript* or any consequences arising from the use of any information it contains.

ROYAL SOCIETY OF CHEMISTRY

www.rsc.org/dalton

View Article Online
DOI: 10.1039/C5DT00433K

Dalton Transactions

RSCPublishing

ARTICLE

# Ruthenium catalysts bearing a benzimidazol-ylidene ligand for the metathetical ring-closure of tetrasubstituted cycloolefins

Cite this: DOI: 10.1039/x0xx00000x

Yannick Borguet,[a] Guillermo Zaragoza,[b] Albert Demonceau[a] and Lionel Delaude*[a]

Received 00th January 2012,
Accepted 00th January 2012

DOI: 10.1039/x0xx00000x

www.rsc.org/

Deprotonation of 1,3-di(2-tolyl)benzimidazolium tetrafluoroborate with a strong base afforded 1,3-di(2-tolyl)benzimidazol-2-ylidene (BTol), which dimerized progressively into the corresponding dibenzotetraazafulvalene. The complexes [RhCl(COD)(BTol)] (COD is 1,5-cyclooctadiene) and *cis*-[RhCl(CO)$_2$(BTol)] were synthesized to probe the steric and electronic parameters of BTol. Comparison of the percentage of buried volume (%$V_{Bur}$) and of the Tolman electronic parameter (TEP) of BTol with those determined previously for 1,3-dimesitylbenzimidazol-2-ylidene (BMes) revealed that the two *N*-heterocyclic carbenes displayed similar electron donicities, yet the 2-tolyl substituents took a slightly greater share of the rhodium coordination sphere than the mesityl groups, due to a more pronounced tilt. The *anti,anti* conformation adopted by BTol in the molecular structure of [RhCl(COD)(BTol)] ensured nonetheless a remarkably unhindered access to the metal center, as evidenced by steric maps. Second-generation ruthenium–benzylidene and isopropoxybenzylidene complexes featuring the BTol ligand were obtained via phosphine exchange from the first generation Grubbs and Hoveyda–Grubbs catalysts, respectively. The atropisomerism of the 2-tolyl substituents within [RuCl$_2$(=CHPh)(PCy$_3$)(BTol)] was investigated by using variable temperature NMR spectroscopy, and the molecular structures of all four possible rotamers of [RuCl$_2$(=CH-*o*-O$^i$PrC$_6$H$_4$)(BTol)] were determined by X-ray crystallography. Both complexes were highly active at promoting the ring-closing metathesis (RCM) of model α,ω-dienes. The replacement of BMes with BTol was particularly beneficial to achieve the ring-closure of tetrasubstituted cycloalkenes. More specifically, the stable isopropoxybenzylidene chelate enabled an almost quantitative RCM of two challenging substrates, *viz.*, diethyl 2,2-bis(2-methylallyl)malonate and *N,N*-bis(2-methylallyl)tosylamide, within a few hours at 60 °C.

## Introduction

Over the past two decades, olefin metathesis has become one of the most powerful tools for the formation of C=C double bonds in polymer chemistry and in organic synthesis.[1,2] The rational design of well-defined molybdenum and ruthenium alkylidene complexes initiated by Schrock[3] and Grubbs[4] in the early 1990s was a crucial milestone in this organometallic success story.[5] Another major leap forward was achieved at the turn of the millennium with the introduction of *N*-heterocyclic carbene (NHC) ligands on ruthenium complexes.[6] As a matter of fact, the so-called second-generation Grubbs (**1**)[7] and Hoveyda–Grubbs (**2**)[8] catalysts stand nowadays as references owing to their high catalytic activity and increased stability compared to their phosphine-based, first-generation analogues (Chart 1).[9]

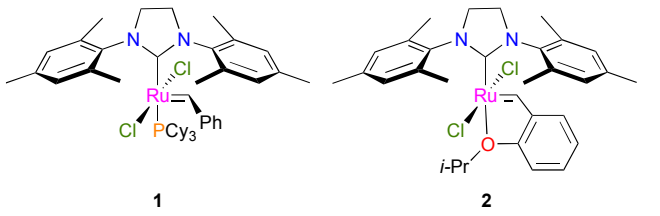


**Chart 1** Second-generation Grubbs and Hoveyda–Grubbs catalysts.

Very recently, tireless catalytic engineering has led to significant advances to further improve the rate of olefin metathesis at low catalyst loading[10] or to achieve high *cis* or *Z* selectivities.[11,12] Despite these spectacular breakthroughs, there are still many hurdles to overcome in order to make olefin metathesis a truly universal catalytic process. In particular, the formation of tetrasubstituted cycloolefins via ring-closing metathesis (RCM) remains a challenging task for most second-

View Article Online
DOI: 10.1039/C5DT00453K
Journal Name



generation catalysts such as **1** or **2**.[13] This is mainly due to the difficulty of coordinating a sterically hindered substrate to a ruthenium active species bearing a bulky NHC ligand such as 1,3-dimesitylimidazolin-2-ylidene (known as SIMes).

A key observation toward the development of efficient catalyst precursors for the RCM of tetrasubstituted cycloolefins was made by Grubbs and co-workers in 2006.[14] During the desymmetrization of a triene in the presence of ruthenium complex **3** bearing a chiral NHC ligand (Chart 2), the unexpected formation of a tetrasubstituted cycloalkene byproduct took place. It was explained by the presence of only one *ortho*-substituent on each *N*-aryl group of the carbene ligand, which reduced the steric pressure around the metal center. Building on this hypothesis, Grubbs *et al.* designed several catalysts with low steric demand, which proved very active for the RCM of challenging tetrasubstituted olefins, but were also quite unstable.[15] This lack of stability was attributed to the free rotation of mono-*ortho* or unsubstituted *N*-aryl moieties around the C–N exocyclic bonds of the NHC ligand, which brings C–H aryl bonds close to the ruthenium center and promotes their activation, ultimately leading to decomposition processes.[16] This assumption was later confirmed by experimental results[17] and theoretical calculations.[18] Subsequent research efforts aimed at optimizing the balance between activity and stability by modulating the various C and N substituents of the NHC ancillary ligand. Catalysts developed along these lines include the chiral ruthenium–benzylidene complex **4** reported by Grisi *et al.*[19] and the chelated isopropoxybenzylidene complex **5** investigated by Grubbs and co-workers (Chart 2).[15b] Both compounds were highly efficient at promoting the RCM of tetrasubstituted olefins under mild reaction conditions. However, their synthesis required multiple, low-yielding steps and, in some instances, the use of not readily available optically active starting materials.

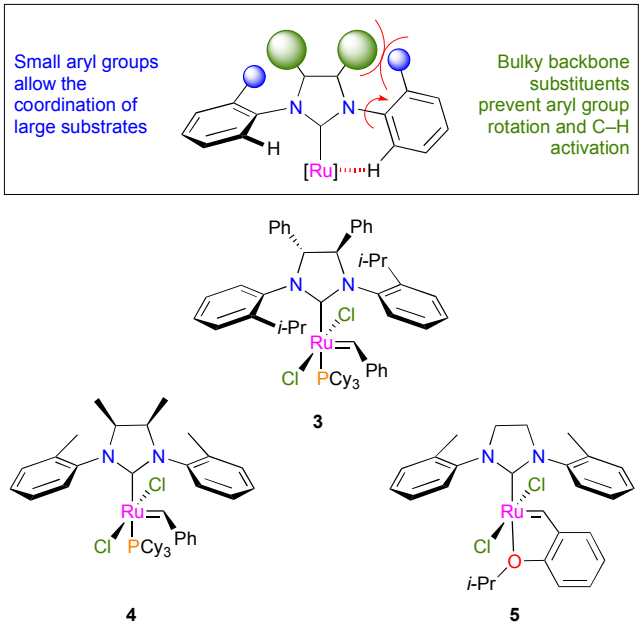


**Chart 2** Second-generation ruthenium–alkylidene catalysts for the RCM of sterically hindered substrates.

As part of our ongoing studies of benzimidazole-based NHCs, we recently assessed the ligand properties of 1,3-dimesitylbenzimidazol-2-ylidene (known as BMes) in ruthenium-catalyzed olefin metathesis reactions.[20] In the benchmark cyclization of diethyl 2,2-diallylmalonate, the [$RuCl_2(PCy_3)$-(BMes)(=CHPh)] complex **6** performed slightly better than the Grubbs second-generation catalyst **1** but gradually lost its catalytic efficiency when model di- and trisubstituted α,ω-dienes were subjected to RCM. These results prompted us to launch further investigations on the 1,3-di(2-tolyl)benzimidazol-2-ylidene ligand (nicknamed BTol). We reasoned that the synergy between small aryl groups on the nitrogen atoms and a bulky fused aromatic ring on the backbone carbon atoms of the central imidazole core should provide an ideal framework for achieving high efficiencies in the RCM of sterically hindered substrates (Chart 3). In this contribution, we first discuss the preparation of suitable precursors for the new BTol ligand and we assess its steric and electronic properties using rhodium complexes. Then, we report on the synthesis of two second-generation ruthenium–alkylidene complexes derived thereof and we probe their catalytic activity in the ring-closing metathesis of various benchmark substrates.

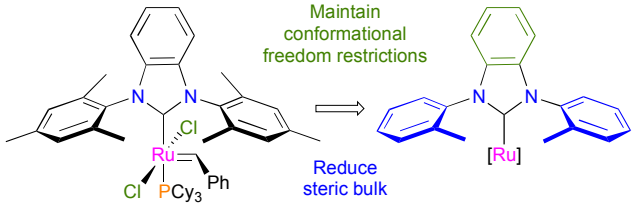


**Chart 3** Tuning of benzimidazole-based ruthenium catalyst **6** for the RCM of sterically hindered substrates.

## Results and discussion

### Synthesis of BTol ligand precursors

Because NHCs are most commonly obtained by deprotonation of the corresponding azolium salts with a strong base,[21] we began our investigations with the preparation of 1,3-di(2-tolyl)-benzimidazolium tetrafluoroborate **7**. Unlike 1,3-dimesitylbenzimidazolium tetrafluoroborate, whose synthesis involved the unexpected formation of a dihydrophenazine intermediate,[22] compound **7** was isolated in high yield following the straightforward amination/cyclization path pioneered by Diver.[23,24] This two-step procedure implied the Buchwald–Hartwig amination of dibromobenzene with *o*-toluidine, followed by a classical formylative cyclization with triethyl orthoformate (Scheme 1). For the sake of convenience, the resulting hygroscopic benzimidazolium chloride was then converted into the corresponding tetrafluoroborate by anion exchange with aqueous tetrafluoroboric acid.[25]

View Article Online
DOI: 10.1039/C5DT00433K


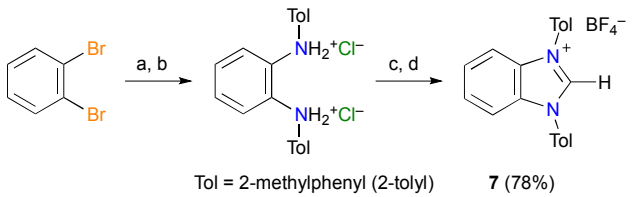


**Scheme 1** Synthesis of 1,3-di(2-tolyl)benzimidazolium tetrafluoroborate (**7**). *Reaction conditions*: (a) *o*-toluidine, $Pd(OAc)_2$, P(*t*-Bu)$_3$, NaO-*t*-Bu, $PhCH_3$, 110 °C, overnight; (b) HCl, $H_2O$; (c) $HC(OEt)_3$, HCl, reflux, overnight; (d) $HBF_4$, $H_2O$.

The deprotonation of salt **7** was carried out with potassium bis(trimethylsilyl)amide in toluene at room temperature. Within 2 h, the initially pale yellow solution became progressively bright orange. This change of color was attributed to the formation of the highly conjugated dibenzotetraazafulvalene **8** in solution (Scheme 2). This observation did not come as a surprise. The dimerization of benzimidazol-2-ylidenes bearing small substituents on their nitrogen atoms is far from unprecedented in the literature.[26] Indeed, these benzannulated carbenes lose less of their aromatic stabilization than imidazol-2-ylidenes when they dimerize. Hence, they exist as dimers at ambient temperature, unless bulky nitrogen substituents shift the equilibrium toward the monomeric NHCs.[27]

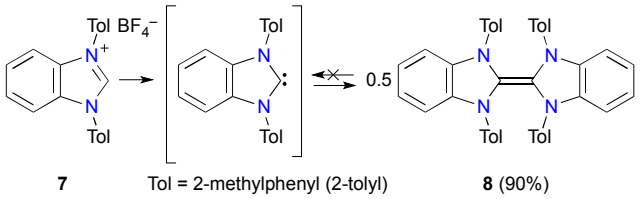


**Scheme 2** Synthesis of the BTol carbene dimer (**8**). *Reaction conditions*: $KN(SiMe_3)_2$, $PhCH_3$, room temp., 2 h.

At room temperature, the $^1$H NMR spectrum of the $(BTol)_2$ dimer **8** featured only poorly resolved signals, a likely indication that the 2-tolyl substituents rotated slowly on the NMR timescale. Warming the sample up to 60 °C led to sharper peaks with discernable coupling patterns between the aromatic protons of the fused benzene ring. $^1$H NMR spectroscopy also revealed the complete disappearance of the singlet originally present at 9.33 ppm in compound **7**, assigned to the acidic proton of the azolium salt starting material. It is noteworthy that the $^{13}$C NMR spectrum recorded at room temperature displayed no resonance within the expected range of chemical shifts for the carbenic carbon of a benzimidazol-2-ylidene (*ca.* 220–230 ppm).[28] Thus, there was no evidence for the intervention of a "Wanzlick equilibrium" between the monomeric free carbene and its dimer,[26b,29] although the poor sensitivity of $^{13}$C NMR for a carbenic carbon devoid of any hydrogen could also account for the lack of signal.

Bright orange crystals of the $(BTol)_2$ dimer **8** suitable for X-ray diffraction analysis were grown by slow evaporation of a saturated solution in toluene under argon. Determination of their molecular structure revealed that the asymmetric unit contained 2.5 molecules of solvent, 0.5 of them distorted around a symmetry element. Within the compound of interest, the C1–C1B distance of 1.347(4) Å between the two monomeric units was similar to those observed in other dibenzotetraazafulvalenes (1.33–1.35 Å).[26b,26d,30] A strong *N*-pyramidalization (average C–N–C angle: 107.5°) and a significant twist around the central $N_2C{=}CN_2$ double bond (average torsion angle: 14.4°) were noticed. These two distortions presumably minimize the steric repulsions between the 2-tolyl substituents.

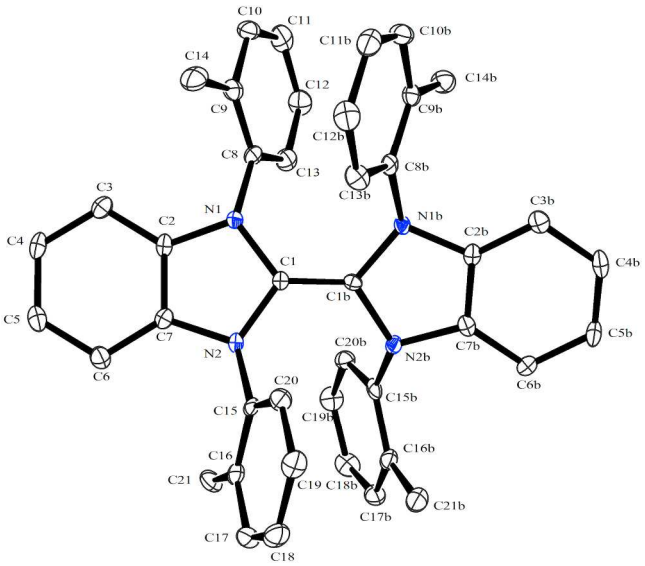


**Fig. 1** ORTEP representation of dibenzotetraazafulvalene **8** with thermal ellipsoids drawn at the 50% probability level. Hydrogen atoms and solvent molecules were removed for clarity. Selected bond length (Å) and angles (°): C1–C1B 1.347(4), N1–C1 1.430(4), N2–C1 1.428(4), N1B–C1B 1.430(4), N2B–C1B 1.435(4); N1–C1–N2 107.4(2), N1B–C1B–N2B 107.6(2), C1–N1–C2 107.0(2), C1B–N1B–C2B 107.1(2), C1–N2–C7 107.4(2), C1B–N2B–C7B 106.9(2).

### Evaluation of the steric and electronic properties of BTol

Among the various complexes that were used to determine the steric and electronic properties of NHC ligands,[31] rhodium derivatives with the generic formulas [RhCl(COD)(NHC)] (COD is 1,5-cyclooctadiene) and *cis*-[RhCl(CO)$_2$(NHC)] are probably the most convenient probes, owing to their straightforward preparation, high stability, and low toxicity.[32] Hence, we first synthesized [RhCl(COD)(BTol)] (**9**) by deprotonating benzimidazolium salt **7** with potassium *tert*-butoxide in the presence of the $[RhCl(COD)]_2$ dimer (Scheme 3). The desired product was isolated as a microcrystalline yellow powder in 82% yield after purification by column chromatography.

View Article Online
DOI: 10.1039/C5DT00453K
Journal Name

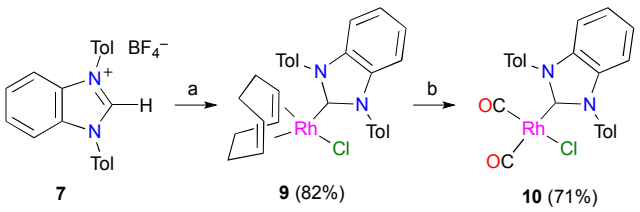


7 9 (82%) 10 (71%)

**Scheme 3** Synthesis of [RhCl(COD)(BTol)] (**9**) and *cis*-[RhCl(CO)$_2$(BTol)] (**10**). *Reaction conditions*: (a) KO-*t*-Bu, [RhCl(COD)]$_2$, THF, room temp., overnight; (b) CO, $CH_2Cl_2$, room temp., 15 min.

$^1$H NMR analysis of [RhCl(COD)(BTol)] (**9**) in $CD_2Cl_2$ at 25 °C showed the presence of three different sets of signals for the *o*-methyl groups of the tolyl substituents (Fig. 2). This is a likely consequence of a restricted rotation around the Rh–NHC and N–Ar bonds.[33] Indeed, there are four possible rotamers for complex **9**, two of them being enantiomers (Chart 4). Based on the X-ray crystal structure discussed below and the relative integrals, we assigned the strongest resonance at 2.02 ppm to the least sterically hindered *anti,anti*-rotamer **9b** and the weakest resonance at 2.29 ppm to the related symmetrical *syn,syn*-rotamer **9a**. The two lines of similar intensities at 2.11 and 2.25 ppm arose from the unsymmetrical *syn,anti* and *anti,syn* pair of enantiomers **9c,d** and the ratios **9a**:**9c,d**:**9b** were of the order of 5:39:56. In the $^{13}C\{^1H\}$ NMR spectrum of complex **11**, only two doublets at 197.9 ($^1J_{Rh-C}$ = 51.1 Hz) and 198.4 ppm ($^1J_{Rh-C}$ = 50.6 Hz) featured a chemical shift and a multiplicity compatible with a carbenic carbon coordinated to a rhodium center. They were assigned to the major rotamers observed on $^1$H NMR spectroscopy. The signal due to **9a** was not detected, probably because of its low intensity or an accidental overlap.

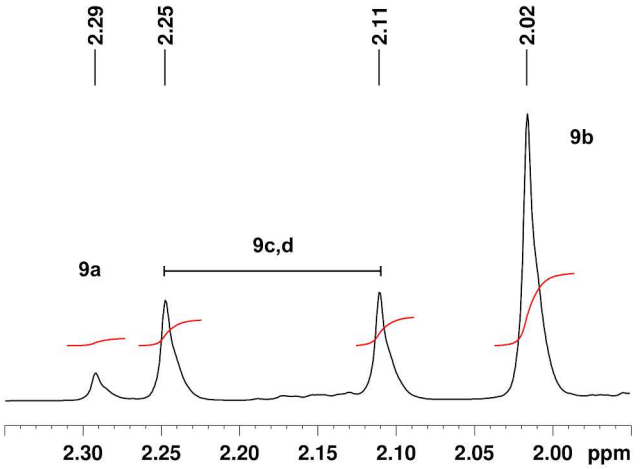


**Fig. 2** $^1$H NMR resonances observed for the *o*-methyl groups of [RhCl(COD)(BTol)] (**9**) in $CD_2Cl_2$ at 298 K (see Chart 4 for the structures of the four possible rotamers).

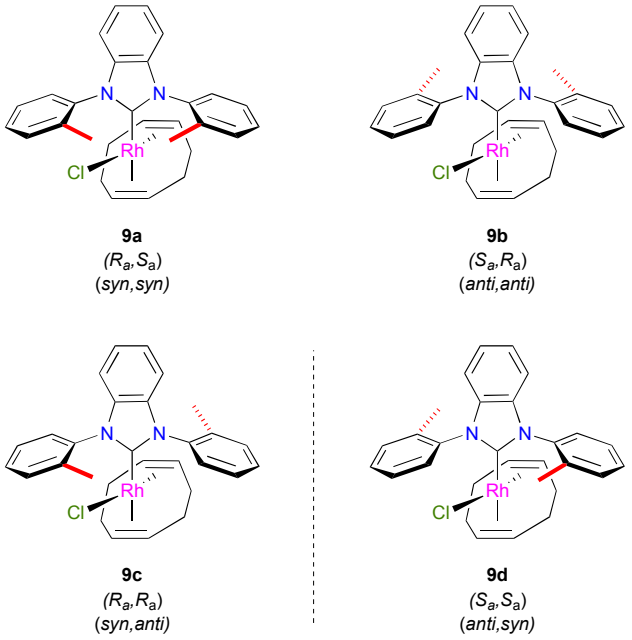


**9a** ($R_a$,$S_a$) (*syn,syn*) **9b** ($S_a$,$R_a$) (*anti,anti*)

**9c** ($R_a$,$R_a$) (*syn,anti*) **9d** ($S_a$,$S_a$) (*anti,syn*)

**Chart 4** Possible rotamers of the [RhCl(COD)(BTol)] complex (**9**) ($R_a$ and $S_a$ absolute configurations refer to the axial chirality of the two exocyclic C–N bonds, *syn* and *anti* descriptors refer to the relative orientations of each methyl group with respect to the chlorido ligand).

Bright yellow crystals of [RhCl(COD)(BTol)] (**9**) suitable for X-ray diffraction analysis were grown by slow evaporation of a concentrated solution in dichloromethane. Only the least sterically hindered *anti,anti*-rotamer **9b** was observed in the solid-state structure, together with one molecule of co-crystallized solvent (Fig. 3). As expected, the ligands adopted a square-planar disposition around the metal center, with the NCN plane of the carbene almost perpendicular to the coordination plane of rhodium. Altogether, the various bond lengths and angles were similar to those reported previously for other complexes of the same family.[20,34] Yet, the tilt angle of the two *o*-tolyl rings in compound **9b** (average value 20°) was significantly more pronounced than the one recorded for mesityl groups in the analogous [RhCl(COD)(BMes)] complex (*ca.* 5°)[20] (Fig. 4). Translated to ruthenium, this should provide an easier access to the metal center, which would be beneficial to the RCM of tetrasubstituted cycloolefins.[35]

View Article Online
DOI: 10.1039/C5DT00453K ARTICLE



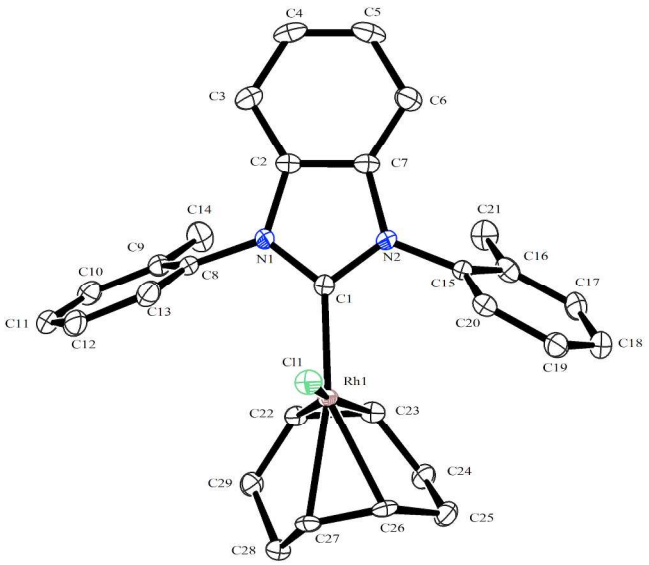


**Fig. 3** ORTEP representation of [RhCl(COD)(BTol)] (**9b**) with thermal ellipsoids drawn at the 50% probability level. Hydrogen atoms and a solvent molecule were removed for clarity. Selected bond length (Å) and angles (°): Rh1–C1 2.003(2), Rh1–Cl1 2.3989(8), Rh1–C22 2.101(3), Rh1–C23 2.112(2), Rh1–C26 2.185(2), Rh1–C27 2.220(2), C1–Rh1–Cl1 90.32(7), N1–C1–N2 105.6(2), C1–N1–C8–C9 111.9(3), C1–N2–C15–C16 −107.5(3).

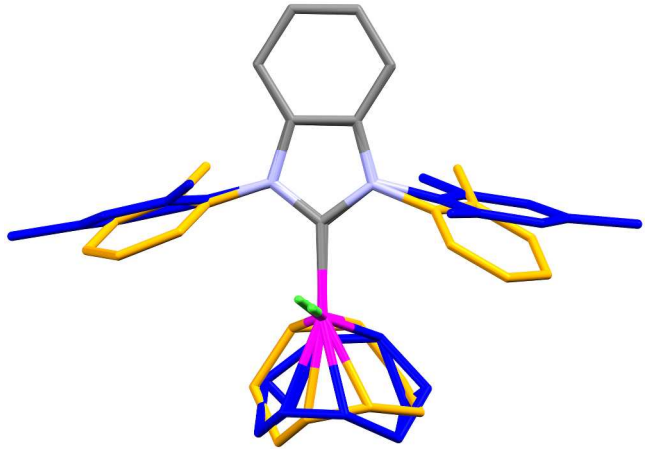

**Fig. 4** Superposition of the molecular structures of [RhCl(COD)(BMes)] (blue) and [RhCl(COD)(BTol)] (**9b**) (yellow).

In order to quantify the steric demand of the BTol ligand, we have extracted its percentage of buried volume (%$V_{Bur}$) from the XRD structure of complex **9b**. This parameter defined by Cavallo and Nolan gives a measure of the space occupied by a ligand in the first coordination sphere of a metal center.[36] It was computed using the web-based application Samb*V*ca.[37] The default processing parameters were kept unchanged (sphere radius: 3.5 Å, distance from the center of the sphere: 2.10 Å, mesh spacing: 0.05 Å, Bondi radii scaled by 1.17, hydrogen atoms omitted). Under these conditions, the BTol ligand exhibited a slightly greater demand than its BMes predecessor, with a %$V_{Bur}$ value of 32.1 *vs.* 30.0.[20] This counterintuitive result can be ascribed to the rotation of the 2-tolyl substituent unhindered side toward the rhodium atom, whereas the mesityl groups are almost perpendicular to the benzimidazole ring and therefore more distant from the metal center (*cf.* Fig. 4).

Steric maps generated using a modified version of the Samb*V*ca program,[35,38] courtesy of Prof. L. Cavallo, provided a more accurate topology of the BMes and BTol ligands in [RhCl(COD)(NHC)] complexes than the %$V_{Bur}$ descriptor. To build the contour plots depicted in Figure 5, the rhodium atom was placed at the origin of a Cartesian coordinate system with the *z* axis corresponding to the Rh–NHC bond and the wingspan of the NHC aligned along the *x* axis. Atom coordinates were extracted from the molecular structures represented in Figures 3 and 4. Positive values of the isocontour lines refer to the top half coordination sphere of the metal center, while the bulk of the NHC ligand resides in the bottom half. Using these conventions, the northern and southern poles of the map computed for the BMes ligand are both strongly shielded by the mesityl groups. Contrastingly, access to the metal via the southern pole is remarkably unhindered with the *anti,anti* conformation adopted by BTol in the solid state structure of [RhCl(COD)(BTol)] (**9b**). Of course, this analysis does not take into account the chlorido and cyclooctadiene ligands, which were removed for the calculations.

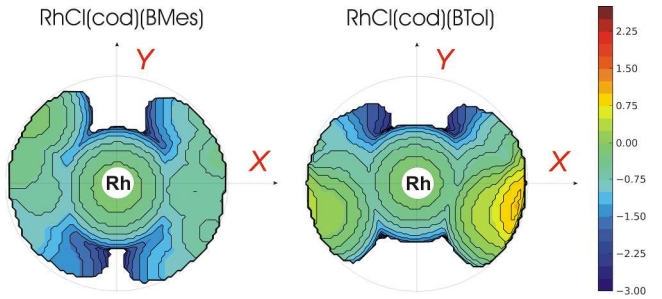


**Fig. 5** %$V_{Bur}$ maps of [RhCl(COD)(BMes)] (left) and [RhCl(COD)(BTol)] (**9b**) (right) with the color scale used to display the isocontour levels (in Å).

Bubbling carbon monoxide into a dichloromethane solution of [RhCl(COD)(BTol)] (**9**) for 15 min at room temperature induced the displacement of the $\eta^4$-diene ligand and afforded the *cis*-dicarbonyl complex **10** in 71% yield (Scheme 3). This product was dissolved again in $CH_2Cl_2$ to record its IR spectrum between NaCl plates. The Tolman electronic parameter (TEP) of BTol was then computed from the average stretching vibration wavenumber of the carbonyl ligands ($\nu_{CO}$ = 2039.5 $cm^{-1}$) using the linear regression proposed by Dröge and Glorius to correlate data obtained from rhodium complexes with the standard nickel-based TEP scale.[39] This led to a corrected value of 2051.8 $cm^{-1}$ for BTol, whereas it was 2052.2 $cm^{-1}$ for BMes.[20] Thus, the electron-donating properties of both *N,N'*-diarylbenzimidazolylidene species were identical within the experimental error range (1 $cm^{-1}$). This result is not surprising, considering that an almost perpendicular orientation of the aryl substituents with respect to the central heterocycle should restrain the transmission of electronic effects from the side-rings to the carbene center. Electrochemical measurements could help better discriminate the two NHCs in terms of electron-donor ability, as they are often more sensitive than IR-

View Article Online
DOI: 10.1039/C5DT00453K
Journal Name

based analyses,[31f,40] but we did not further investigate this option.

### Synthesis of ruthenium complexes

Well-defined metathesis initiators analogous to the second-generation Grubbs (**1**)[7] and Hoveyda–Grubbs (**2**)[8] complexes (*cf.* Chart 1) featuring the BTol ligand were obtained from the corresponding first-generation catalyst precursors via ligand exchange of one tricyclohexylphosphine with a slight excess of NHC generated in situ by deprotonation of 1,3-di(2-tolyl)benzimidazolium tetrafluoroborate (**7**) with potassium bis(trimethylsilyl)amide in toluene (Scheme 4). The synthesis of [$RuCl_2$(=CHPh)($PCy_3$)(BTol)] (**11**) was carried out at room temperature in order to minimize unwanted thermal degradations in solution. Indeed, a rapid decomposition of this ruthenium–benzylidene complex occurred upon heating to 50 °C in toluene. At 20–25 °C, side-reactions were limited and completion was reached within 16 h (overnight). Contrastingly, the synthesis of the more stable isopropoxy-tethered [$RuCl_2$(=CH-*o*-O$^i$Pr$C_6H_4$)(BTol)] complex (**12**) could be achieved within 3 h at 60 °C without noticeable thermal decomposition. In this case, copper(I) chloride was added to the reaction mixture after 1 h to further speed up the transformation.[41]

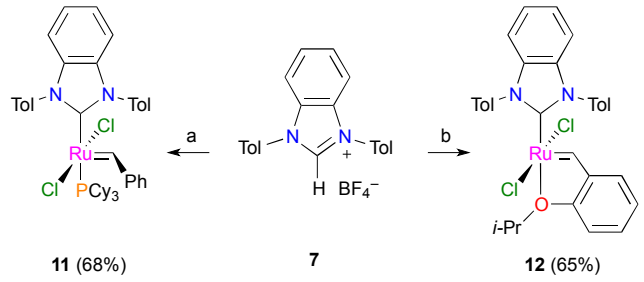


**11** (68%) **7** **12** (65%)

**Scheme 4** Synthesis of second-generation ruthenium–alkylidene complexes **11** and **12**. *Reaction conditions*: (a) $KN(SiMe_3)_2$, [$RuCl_2$(=CHPh)($PCy_3$)$_2$], $PhCH_3$, room temp., overnight; (b) $KN(SiMe_3)_2$, [$RuCl_2$(=CH-*o*-O$^i$Pr$C_6H_4$)($PCy_3$)], $PhCH_3$, 60 °C, 1 h then CuCl, 60 °C, 2 h.

The enhanced stability of complex **12** compared to **11** was also evidenced during the work-up of the reactions. Purification of the yellow-green chelate **12** by column chromatography on silica gel could be performed with no particular precautions under a normal atmosphere. On the other hand, the red-brown compound **11** could only be isolated with a satisfactory yield when elution was carried out under an inert atmosphere with dry and degassed solvents.

The identity and the purity of [$RuCl_2$(=CHPh)($PCy_3$)(BTol)] (**11**) were established by various analytical techniques. It should be pointed out that there are eight possible rotamers for this complex, divided into two groups of four diastereoisomers, which are non superimposable mirror images of each other (Chart 5). They arise from the restricted rotation of the 2-tolyl substituents within the BTol ligand in conjunction with the asymmetric nature of the Ru=CHPh fragment. Only two sets of signals were visible in the multinuclear NMR spectra recorded in $CD_2Cl_2$ at 25 °C. Thus, on $^1$H NMR spectroscopy, the benzylidene protons of complex **11** resonated as two singlets centered at 19.26 and 19.22 ppm in a 6:4 ratio (Fig. 6, left). In line with this observation, two signals in a 4:6 ratio were also present at 29.23 and 26.22 ppm in the $^{31}$P{$^1$H} NMR spectrum acquired at the same temperature (Fig. 7, left), while the $^{13}$C{$^1$H} spectrum featured two highly deshielded absorptions for the benzylidene carbenic carbons at 297.3 and 294.5 ppm, respectively. All these assignments were confirmed by using standard COSY, DEPT, HMBC and HSQC sequences, but we did not further investigate through-space interactions between the various stereogenic units of complex **11** via 2D-NOESY or other advanced NMR techniques.

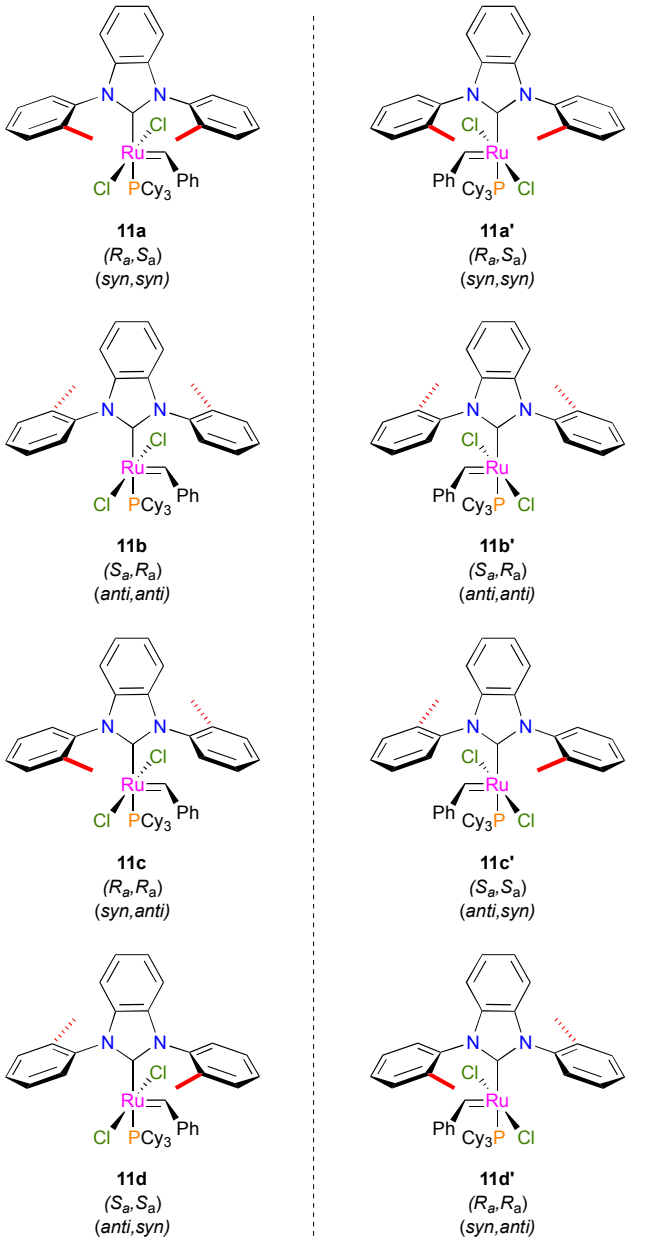


**Chart 5** Possible rotamers of the [$RuCl_2$(=CHPh)($PCy_3$)(BTol)] complex (**11**) ($R_a$ and $S_a$ absolute configurations refer to the axial chirality of the two exocyclic C–N

Journal Name

View Article Online
DOI: 10.1039/C5DT00453K ARTICLE

bonds, *syn* and *anti* descriptors refer to the relative orientations of each methyl group with respect to the benzylidene unit).

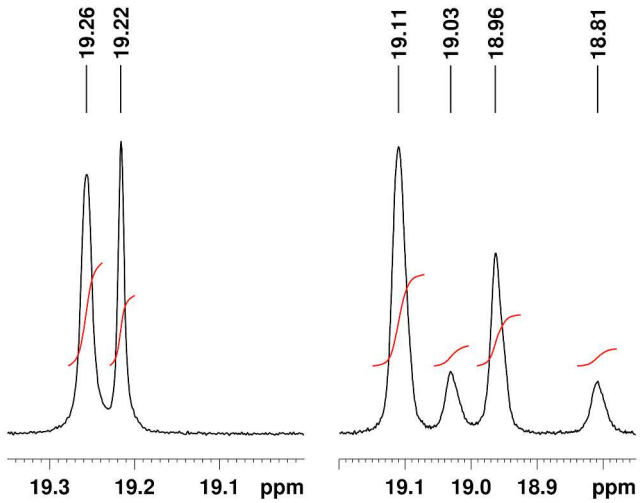


**Fig. 6** $^{1}$H NMR resonances of the benzylidene proton in [$RuCl_2$(=CHPh)($PCy_3$)-(BTol)] (**11**) dissolved in $CD_2Cl_2$ at 298 K (left) and 223 K (right).

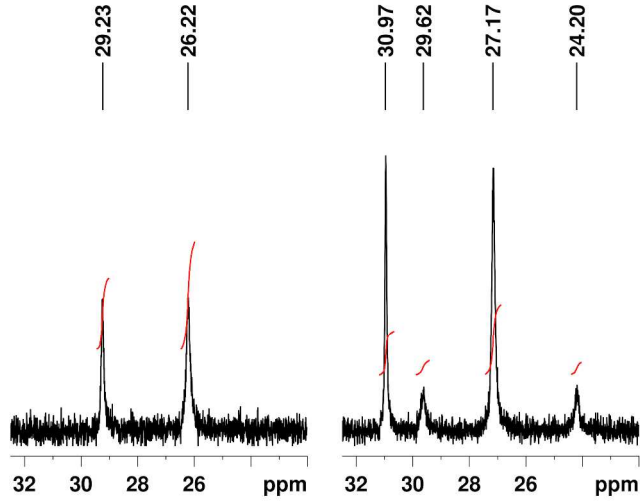


**Fig. 7** $^{31}P\{^{1}H\}$ NMR resonances of the $PCy_3$ ligand in [$RuCl_2$(=CHPh)($PCy_3$)(BTol)] (**11**) dissolved in $CD_2Cl_2$ at 298 K (left) and 223 K (right).

We tentatively assume that the rotation of the 2-tolyl substituent located above the benzylidene fragment should be hindered, while the other *N*-aryl substituent could rotate freely at 25 °C, thereby leading to the two observed conformations. Alternatively, a rotation of the BTol ligand around the Ru–NHC axis could also justify the observation of two sets of NMR signals, as it would equilibrate the (*syn,syn*) and (*anti,anti*) atropisomers on one hand, and their (*syn,anti*) and (*anti,syn*) counterparts on the other hand. All the variable temperature NMR investigations carried out so far to determine rotational barriers within second-generation complexes of type **1** concluded, however, to an easier interconversion of two rotational isomers around a N–aryl bond than around the Ru–NHC axis.[42]

When the temperature was lowered to –50 °C, all the rotation modes could be frozen and four sets of signals became clearly visible in the $^{1}$H and $^{31}P\{^{1}H\}$ NMR spectra of complex **11**. Indeed, the two resonances originally detected at 19.26 and 19.22 ppm for the benzylidene protons were further split into four singlets and slightly shifted to lower field upon cooling (Fig. 6, right). Hence, their chemical shifts were 19.11, 19.03, 18.96 and 18.81 ppm and the integral ratios were 5:1:3:1. Likewise, the $^{31}P\{^{1}H\}$ NMR spectrum of [$RuCl_2$(=CHPh)-($PCy_3$)(BTol)] (**11**) recorded at –50 °C featured four separate singlets for the phosphine ligand at 30.97, 29.62, 27.17, and 24.20 ppm with the proportions 3:1:5:1 (Fig. 7, right). These data provide unambiguous experimental evidence for the formation of racemic mixtures containing two major and two minor rotamers, but a more specific assignment of each resonance to structures **11a–d/11a'–d'** was not carried out.

Despite numerous attempts, we were not able to isolate crystals of the ruthenium-benzylidene complex **11** suitable for X-ray diffraction analysis. This is most likely due to the limited stability of this compound in solution. In the case of chelated species **12**, on the other hand, we were very pleased to observe the formation of two distinct types of crystals during a slow recrystallization process at room temperature. Crystals of type **A** were found to contain the ($S_a$,$R_a$) and ($S_a$,$S_a$)-rotamers **12b** and **12d** co-crystallized in the same unit cell in a 6:4 ratio. Conversely, crystals of type **B** mostly consisted of the ($R_a$,$R_a$)-rotamer **12c** with a 20% disorder due to the joint presence of the ($R_a$,$S_a$)-conformer **12a** (Fig. 8). Thus, we were able to determine the molecular structure of all four possible stereoisomers of [$RuCl_2$(=CH-*o*-O$^{i}$Pr$C_6H_4$)(BTol)] (**12**). It should be pointed out that crystals **A** and **B** were not true enantiomers, because the two diastereoisomers in each of them were not in the same proportions. Yet, there might exist other crystals in the sample with different diastereoisomeric ratios. As a matter of fact, both crystals **A** and **B** were monoclinic and belonged to similar space groups that are interchangeable by a slight metric adaptation ($P2_1/c$ and $P2_1/n$, respectively).

View Article Online
DOI: 10.1039/C5DT00453K
Journal Name



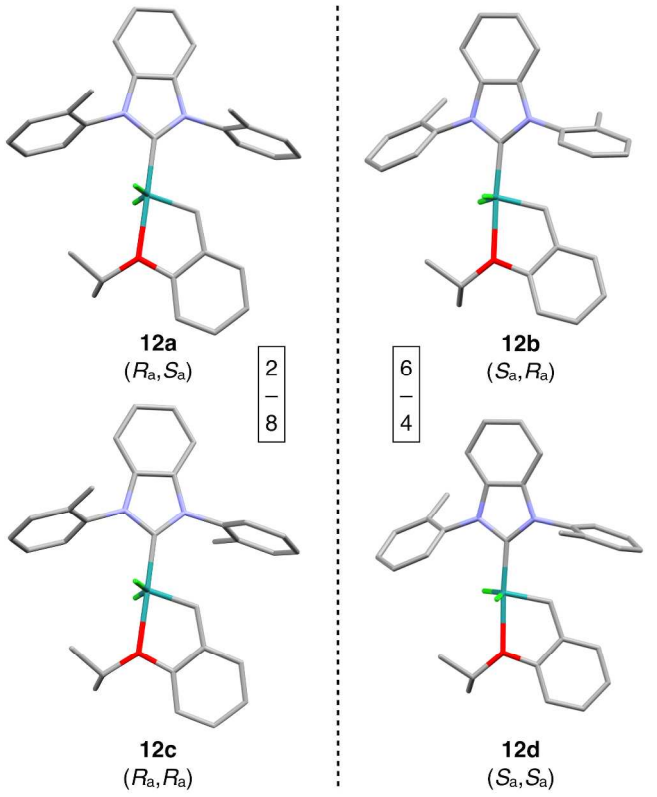


**Fig. 8** Molecular structures of [$RuCl_2$(=CH-*o*-$O^iPrC_6H_4$)(BTol)] (**12**) derived from the two types of crystals obtained ($R_a$ and $S_a$ absolute configurations refer to the axial chirality of the two exocyclic C–N bonds).

In both crystal forms, the 2-tolyl substituent located above the isopropoxybenzylidene unit could adopt two distinct orientations, whereas the other *N*-aryl group was well-refined in a single position. Strong intramolecular hydrogen bonds with the chlorine atoms might explain this lock. Conversely, when the aromatic ring of the 2-tolyl substituent is located above the benzylidene proton, there is a competition between the formation of H···Cl bonds and C–H···π interactions (see ESI for details). The ruthenium atom was pentacoordinated and displayed a distorted square-pyramidal geometry. As expected, the two chlorine atoms were located trans to each other in the basal plane, while the two other mutual trans positions were occupied by the chelating oxygen of the isopropoxy group and the carbenic carbon of the BTol ligand. The benzylidene unit took up the apical position and its aromatic part was almost coplanar with the benzimidazole fused rings. Bond lengths and angles were in line with those reported previously for various other second-generation Hoveyda–Grubbs catalysts.[16,19a,43]

A key structural feature is that the 2-tolyl group located below the basal plane was significantly more tilted than the one above the apical benzylidene unit for obvious steric reasons. Thus, the average deviations from perpendicularity to the benzimidazole ring were, respectively, 24° and 3° in **12a** and **12c**, 31° and 9° in **12d**, and 31° and 23° in **12b**. The discrepancy between the values measured for the last two diastereoisomers in crystal **A** is reminiscent of a similar case reported by Grubbs *et al.* when they determined the molecular structure of [$RuCl_2$(=CH-*o*-$O^iPrC_6H_4$)(SITol)] (**5**) (SITol is 1,3-di(2-tolyl)imidazolin-2-ylidene).[15b,43d] The single crystal of this compound featured two conformers analogous to **12b** and **12d** in a 91:9 ratio. In the major syn rotamer, the 2-tolyl substituent below the basal plane was rotated 35° away from being orthogonal to the NHC plane, while the other one lay within 5° of perpendicularity. In the minor anti rotamer, these angles became 35° and 16°, respectively. Of note, the tilt of the mesityl groups in the original second-generation Hoveyda–Grubbs catalyst (**2**) were 6° and 9°.[8] Both complexes **5** and **12** should therefore provide additional space near the ruthenium center to accommodate large incoming substrates.

In order to investigate more thoroughly the steric requirements of BTol, we have extracted its $\%V_{Bur}$ parameter from the molecular structures of **12b** and **12c**. In these two major conformers, the relative orientation of the *ortho*-methyl groups (syn or anti, *cf.* Fig. 8) did not seem to have any influence on $\%V_{Bur}$ and led to values of 30.3 and 30.2, respectively, down from 32.1 in rhodium complex **9b**. These variations demonstrate once again the structural flexibility of NHCs and their ability to fit with the crowding around a metal center.[35,36d] A more informative comparison was made with the original Hoveyda–Grubbs catalyst **2**, in which the SIMes ligand occupied 31.7[8a] or 31.8%[44] of the ruthenium coordination sphere, depending on the crystal structure used to perform the calculations. Of course, all these tilt angles and buried volumes may overestimate actual angle compressions in a solution, which is free of crystal packing forces.

### Catalytic tests

Complexes **11** and **12** were tested as catalyst precursors for the RCM of four model α,ω-dienes. Standard benchmark conditions defined by Grubbs and co-workers were applied to ease the comparison with various other second-generation catalysts featuring mesityl-substituted NHC ligands.[45] We first investigated the RCM of diethyl diallylmalonate (DEDAM, **13**) in $CD_2Cl_2$ at 30 °C (Scheme 5). Reactions were carried out using 1 mol% of ruthenium initiator and monitored by $^1$H NMR spectroscopy. Under these conditions, an almost quantitative conversion of the substrate into cyclopentene diester **14** occurred within 40 min with [$RuCl_2(PCy_3)$(BMes)(=CHPh)] (**6**) (Fig. 9). Previous work had already established that this BMes-based initiator and the original Grubbs second-generation catalyst **1** displayed similar reactivities in the RCM of the model disubstituted cycloolefin under examination.[20] Replacement of BMes or SIMes with BTol on the ruthenium–benzylidene scaffold led to a slight rate enhancement. Conversely, 2 h were needed to reach completion with the isopropoxybenzylidene complex **12**, whereas the Hoveyda–Grubbs catalyst **2** was reported to keep an almost unchanged activity compared to **1**.[45,46]

Journal Name

View Article Online
DOI: 10.1039/C5DT00453K ARTICLE

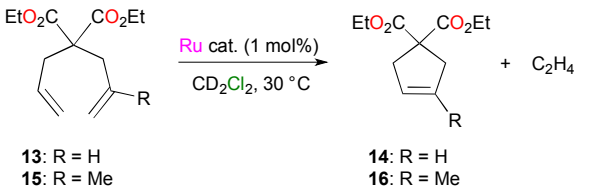


**13**: R = H
**15**: R = Me

**14**: R = H
**16**: R = Me

**Scheme 5** Ruthenium-catalyzed RCM of diethyl 2,2-diallylmalonate (**13**) and diethyl 2-allyl-2-(2-methylallyl)malonate (**15**).

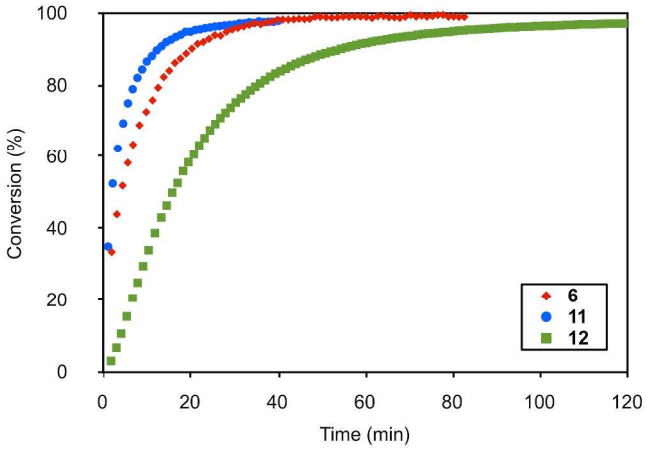


**Fig. 9** Time course of the RCM of diethyl 2,2-diallylmalonate (**13**) catalyzed by [$RuCl_2(PCy_3)$(BMes)(=CHPh)] (**6**), [$RuCl_2(PCy_3)$(BTol)(=CHPh)] (**11**), and [$RuCl_2$(=CH-*o*-O$^i$Pr$C_6H_4$)(BTol)] (**12**) (1 mol% in $CD_2Cl_2$ at 30 °C).

The reduced initiation efficiency of chelate **12** compared to the mixed phosphine/NHC complexes **6** and **11** became even more obvious when the RCM of diethyl 2-allyl-2-(methylallyl)-malonate (**15**) was carried out in $CD_2Cl_2$ at 30 °C (Scheme 5 and Fig. 10). When 1 mol% of benzylidene catalyst **11** was added to the reaction mixture, conversion climbed to 90% within an hour, but then started to level off and ultimately stopped at 95% after 2 h. Complex **6**, on the other hand, remained active for a longer period of time and afforded a quantitative yield of trisubstituted cycloolefin **16** within 3 h. A different pattern was observed with chelate **12**, which suggested a short induction period at the onset of the reaction, followed by a slow, albeit steady, progress that led to a 74% conversion after 2 h. The 90% threshold was reached after 3.5 h and no sign of deactivation was detected at that point. Yet, the experiment was not prolonged to reach full conversion.

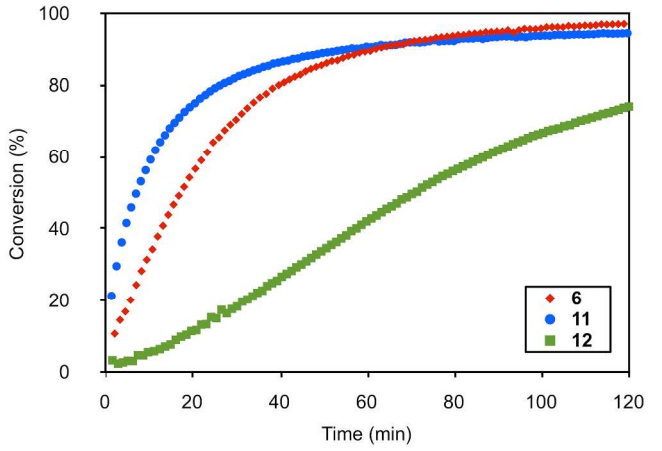


**Fig. 10** Time course of the RCM of diethyl 2-allyl-2-(2-methylallyl)malonate (**15**) catalyzed by [$RuCl_2(PCy_3)$(BMes)(=CHPh)] (**6**), [$RuCl_2(PCy_3)$(BTol)(=CHPh)] (**11**), and [$RuCl_2$(=CH-*o*-O$^i$Pr$C_6H_4$)(BTol)] (**12**) (1 mol% in $CD_2Cl_2$ at 30 °C).

Next, we examined the RCM of the two sterically demanding α,ω-dienes **17** and **19** derived from diethyl malonate and tosylamide, respectively (Scheme 6). Standard benchmark conditions for these challenging substrates implied the recourse to 5 mol% of catalyst.[45] Previous assessment of [$RuCl_2(PCy_3)$-(BMes)(=CHPh)] (**6**) in toluene-$d_8$ at 80 °C had shown that the BMes-benzylidene complex was largely inefficient at promoting the RCM of tetrasubstituted cycloalkenes.[20] Despite a strong thermal activation, it did not afford satisfactory yields of cycloproducts **18** and **20** and was completely deactivated in less than 10 min (Figures 11 and 12). Very gratifyingly, its BTol analogue **11** was much more effective for inducing the same transformations in $CD_2Cl_2$ at 30 °C. With this catalyst precursor, conversion reached 84% after 2 h with the dimethallylmalonate **17** and 90% with the slightly more reactive tosylamide **19**. Extending the reaction time did not further increase the yield of **18** and brought the conversion to a final value of 93% within 3 h in the case of **20**. To further improve these results, we decided to test the chelated isopropoxybenzylidene complex **12** in benzene-$d_6$ at 60 °C. We reasoned that a thermal activation would compensate for the slow initiation tendency displayed by this chelate in the RCM of diesters **13** and **14**. Indeed, the temperature increase combined with the reduced steric bulk of the BTol ligand compared to BMes or SIMes allowed to fully convert substrate **19** into cyclic product **20** in less than 2 h, thereby demonstrating the validity of our approach. In the case of diester **17**, a short induction period of about 15 min was observed before the reaction took off and a 84% conversion was recorded after 2 h. it kept slowly increasing and product **18** was eventually obtained in 96% yield after 4 h.

View Article Online
DOI: 10.1039/C5DT00453K
Journal Name

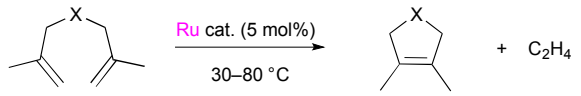


**17**: X = $C(CO_2Et)_2$
**19**: X = NTs
**18**: R = $C(CO_2Et)_2$
**20**: X = NTs

**Scheme 6** Ruthenium-catalyzed RCM of diethyl 2,2-bis(2-methylallyl)malonate (**17**) and *N,N*-bis(2-methylallyl)tosylamide (**19**).

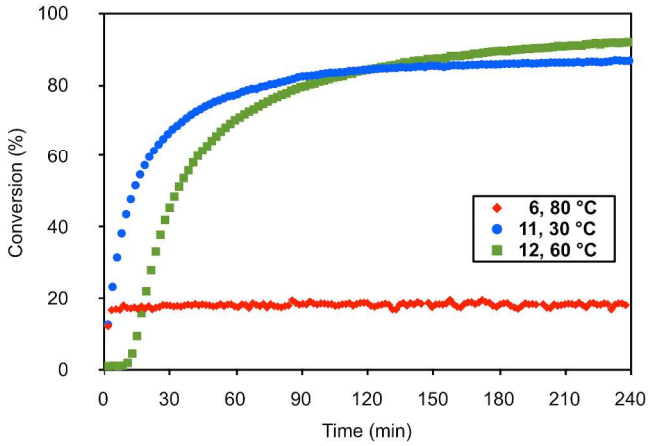


**Fig. 11** Time course of the RCM of diethyl 2,2-bis(2-methylallyl)malonate (**17**) catalyzed by $[RuCl_2(PCy_3)(BMes)(=CHPh)]$ (**6**) (5 mol% in $C_6D_5CD_3$ at 80 °C), $[RuCl_2(PCy_3)(BTol)(=CHPh)]$ (**11**) (5 mol% in $CD_2Cl_2$ at 30 °C), and $[RuCl_2(=CH\text{-}o\text{-}O^iPrC_6H_4)(BTol)]$ (**12**) (5 mol% in $C_6D_6$ at 60 °C).

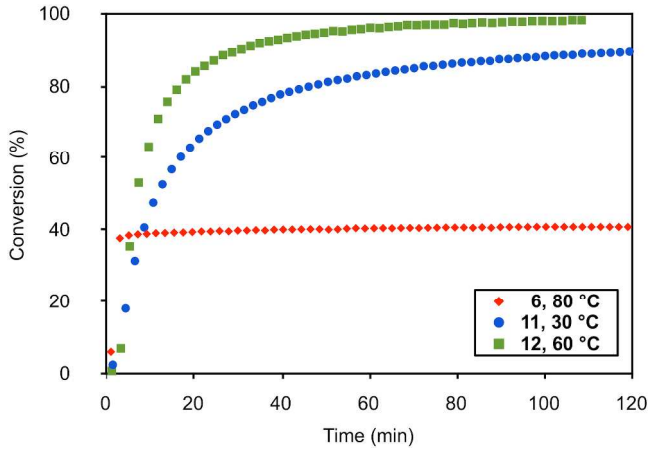


**Fig. 12** Time course of the RCM of *N,N*-bis(2-methylallyl)tosylamide (**19**) catalyzed by $[RuCl_2(PCy_3)(BMes)(=CHPh)]$ (**6**) (5 mol% in $C_6D_5CD_3$ at 80 °C), $[RuCl_2(PCy_3)(BTol)(=CHPh)]$ (**11**) (5 mol% in $CD_2Cl_2$ at 30 °C), and $[RuCl_2(=CH\text{-}o\text{-}O^iPrC_6H_4)(BTol)]$ (**12**) (5 mol% in $C_6D_6$ at 60 °C).

## Conclusion and perspectives

1,3-Di(2-tolyl)benzimidazolium tetrafluoroborate **7** was easily obtained via the amination/cyclization of 1,2-dibromobenzene. Deprotonation of this benzimidazolium salt with a strong base afforded the new *N*-heterocyclic carbene BTol, which was found to dimerize progressively into the corresponding dibenzotetraazafulvalene **8**. Coordination of BTol to rhodium or ruthenium further led to a small, albeit representative, set of new organometallic products. Comparison of the $\%V_{Bur}$ and TEP values computed for BTol in [RhCl(COD)(BTol)] (**9**) and *cis*-$[RhCl(CO)_2(BTol)]$ (**10**), respectively, with those determined previously from the analogous rhodium complexes of BMes revealed that the two NHCs displayed similar electron donicities. Yet, the 2-tolyl substituents took a slightly greater share of the rhodium coordination sphere than the mesityl groups, due to a more pronounced tilt. The *anti,anti* conformation adopted by BTol in the molecular structure of complex **9b** ensured nonetheless a remarkably unhindered access to the metal center, as evidenced by the examination of steric maps.

Second-generation ruthenium–benzylidene and ruthenium–isopropoxybenzylidene complexes **11** and **12** featuring the new BTol ligand were synthesized via phosphine exchange from the first generation Grubbs and Hoveyda–Grubbs catalysts, respectively. The atropisomerism of the 2-tolyl substituents within the $[RuCl_2(=CHPh)(PCy_3)(BTol)]$ complex (**11**) was investigated by using variable temperature $^1H$ and $^{31}P$ NMR spectroscopies, and the molecular structures of all four possible rotamers of $[RuCl_2(=CH\text{-}o\text{-}O^iPrC_6H_4)(BTol)]$ (**12**) were determined by X-ray crystallography. Both complexes were highly active at promoting the RCM of model α,ω-dienes. In line with our expectations, the replacement of BMes with BTol was particularly beneficial to achieve the ring-closure of tetrasubstituted cycloalkenes. More specifically, the stable chelate **12** enabled an almost quantitative RCM of two challenging substrates, *viz.*, diethyl dimethallylmalonate (**17**) and *N,N*-dimethallyltosylamide (**19**), within a few hours at 60 °C.

To sum up, we have demonstrated that 1,3-di(2-tolyl)benzimidazol-2-ylidene (BTol) was a very suitable NHC ligand for achieving the RCM of tetrasubstituted cycloolefins using second-generation ruthenium–alkylidene catalysts. Furthermore, the synthesis of this new ancillary ligand proceeded with remarkable ease, as it required only three steps, among which one was catalytic, from widely available starting materials. Further investigations are in progress to evaluate more thoroughly the efficiency of complexes **11** and **12** in the RCM of a wide range of α,ω-dienes, and to compare their activities and stabilities with those of commercially available catalysts such as **5**. Details of these experiments will be reported in due course.

## Acknowledgements

The financial support of the "Fonds de la Recherche Scientifique–FNRS", Brussels, through grant J.0058.13 is gratefully acknowledged. The authors would like to thank Prof. Luigi Cavallo and Dr. Laura Falivene, University of Salerno, Italy, for generating the steric maps depicted in Figures 5 and S4.

## Notes and references

View Article Online
DOI: 10.1039/C5DT00455K ARTICLE

[a] Laboratory of Organometallic Chemistry and Homogeneous Catalysis, Institut de Chimie (B6a), Université de Liège, Sart-Tilman par 4000 Liège, Belgium. E-mail: l.delaude@ulg.ac.be; http://www.cata.ulg.ac.be
[b] Unidade de Difracción de Raios X, Edificio CACTUS, Universidade de Santiago de Compostela, Campus Vida, 15782 Santiago de Compostela, Spain

† Electronic Supplementary Information (ESI) available: Experimental procedures, detailed crystallographic analysis of compounds **8**, **9**, and **12**, $^{1}$H, $^{13}$C, and $^{31}$P NMR spectra of all the new compounds. CCDC 1045783–1045786. For ESI and crystallographic data in CIF or other electronic format see DOI: 10.1039/b000000x/

1 For monographs, see: (*a*) *Handbook of Metathesis*, ed. R. H. Grubbs, Wiley-VCH, Weinheim, 2003; (*b*) *Green Metathesis Chemistry*, NATO Science for Peace and Security Series-A: Chemistry and Biology, ed. V. Dragutan, A. Demonceau, I. Dragutan and E. S. Finkelshtein, Springer, Dordrecht, 2010; (*c*) *Metathesis in Natural Product Synthesis: Strategies, Substrates and Catalysts*, ed. J. Cossy, S. Arseniyadis and C. Meyer, Wiley-VCH, Weinheim, 2010; (*d*) *Olefin Metathesis: Theory and Practice*, ed. K. Grela, John Wiley & Sons, Hoboken, NJ, 2014.

2 For selected reviews, see: (*a*) A. Fürstner, *Angew. Chem. Int. Ed.*, 2000, **39**, 3012–3043; (*b*) M. R. Buchmeiser, *Chem. Rev.*, 2000, **100**, 1565–1604; (*c*) S. J. Connon and S. Blechert, *Angew. Chem. Int. Ed.*, 2003, **42**, 1900–1923; (*d*) A. Deiters and S. F. Martin, *Chem. Rev.*, 2004, **104**, 2199–2238; (*e*) C. Slugovc, *Macromol. Rapid Commun.*, 2004, **25**, 1283-1297; (*f*) K. C. Nicolaou, P. G. Bulger and D. Sarlah, *Angew. Chem. Int. Ed.*, 2005, **44**, 4490–4527; (*g*) N. Holub and S. Blechert, *Chem. Asian J.*, 2007, **2**, 1064–1082; (*h*) A. H. Hoveyda and A. R. Zhugralin, *Nature*, 2007, **450**, 243–251; (*i*) W. A. L. van Otterlo and C. B. de Koning, *Chem. Rev.*, 2009, **109**, 3743–3782; (*j*) S. Monfette and D. E. Fogg, *Chem. Rev.*, 2009, **109**, 3783–3816.

3 (*a*) R. R. Schrock, *Acc. Chem. Res.*, 1990, **23**, 158–165; (*b*) R. R. Schrock and A. H. Hoveyda, *Angew. Chem. Int. Ed.*, 2003, **42**, 4592–4633.

4 (*a*) T. M. Trnka and R. H. Grubbs, *Acc. Chem. Res.*, 2001, **34**, 18–29; (*b*) R. H. Grubbs, *Tetrahedron*, 2004, **60**, 7117–7140.

5 (*a*) D. Astruc, *New J. Chem.*, 2005, **29**, 42–56; (*b*) T. J. Katz, *New J. Chem.*, 2006, **30**, 1844–1847; (*c*) D. Astruc, *New J. Chem.*, 2006, **30**, 1848–1852; (*d*) C. Deraedt, M. d'Halluin and D. Astruc, *Eur. J. Inorg. Chem.*, 2013, 4881–4908.

6 (*a*) M. Scholl, T. M. Trnka, J. P. Morgan and R. H. Grubbs, *Tetrahedron Lett.*, 1999, **40**, 2247–2250; (*b*) T. Weskamp, F. J. Kohl, W. Hieringer, D. Gleich and W. A. Herrmann, *Angew. Chem. Int. Ed.*, 1999, **38**, 2416–2419; (*c*) L. Ackermann, A. Fürstner, T. Weskamp, F. J. Kohl and W. A. Herrmann, *Tetrahedron Lett.*, 1999, **40**, 4787–4790; (*d*) J. Huang, H.-J. Schanz, E. D. Stevens and S. P. Nolan, *Organometallics*, 1999, **18**, 5375–5380.

7 (*a*) M. Scholl, S. Ding, C. W. Lee and R. H. Grubbs, *Org. Lett.*, 1999, **1**, 953–956; (*b*) T. M. Trnka, J. P. Morgan, M. S. Sanford, T. E. Wilhelm, M. Scholl, T.-L. Choi, S. Ding, M. W. Day and R. H. Grubbs, *J. Am. Chem. Soc.*, 2003, **125**, 2546–2558.

8 (*a*) S. B. Garber, J. S. Kingsbury, B. L. Gray and A. H. Hoveyda, *J. Am. Chem. Soc.*, 2000, **122**, 8168–8179; (*b*) S. Gessler, S. Randl and S. Blechert, *Tetrahedron Lett.*, 2000, **41**, 9973–9976.

9 (*a*) P. H. Deshmukh and S. Blechert, *Dalton Trans.*, 2007, 2479–2491; (*b*) C. Samojłowicz, M. Bieniek and K. Grela, *Chem. Rev.*, 2009, **109**, 3708–3742; (*c*) G. C. Vougioukalakis and R. H. Grubbs, *Chem. Rev.*, 2010, **110**, 1746–1787; (*d*) F. B. Hamad, T. Sun, S. Xiao and F. Verpoort, *Coord. Chem. Rev.*, 2013, **257**, 2274–2292.

10 (*a*) X. Bantreil, T. E. Schmid, R. A. M. Randall, A. M. Z. Slawin and C. S. J. Cazin, *Chem. Commun.*, 2010, **46**, 7115–7117; (*b*) T. E. Schmid, X. Bantreil, C. A. Citadelle, A. M. Z. Slawin and C. S. J. Cazin, *Chem. Commun.*, 2011, **47**, 7060–7062; (*c*) L. H. Peeck, R. D. Savka and H. Plenio, *Chem. Eur. J.*, 2012, **18**, 12845–12853; (*d*) P. Kos, R. Savka and H. Plenio, *Adv. Synth. Catal.*, 2013, **355**, 439–447; (*e*) R. Kadyrov, *Chem. Eur. J.*, 2013, **19**, 1002–1012; (*f*) J. Czaban, B. M. Schertzer and K. Grela, *Adv. Synth. Catal.*, 2013, **355**, 1997–2006; (*g*) M. Abbas, A. Leitgeb and C. Slugovc, *Synlett*, 2013, **24**, 1193–1196.

11 For molybdenum and tungsten catalysts, see: (*a*) A. Córdova and R. Rios, *Angew. Chem. Int. Ed.*, 2009, **48**, 8827–8831; (*b*) D. V. Peryshkov, R. R. Schrock, M. K. Takase, P. Müller and A. H. Hoveyda, *J. Am. Chem. Soc.*, 2011, **133**, 20754–20757; (*c*) M. Yu, I. Ibrahem, M. Hasegawa, R. R. Schrock and A. H. Hoveyda, *J. Am. Chem. Soc.*, 2012, **134**, 2788–2799; (*d*) E. M. Townsend, R. R. Schrock and A. H. Hoveyda, *J. Am. Chem. Soc.*, 2012, **134**, 11334–11337; (*e*) E. T. Kiesewetter, R. V. O'Brien, E. C. Yu, S. J. Meek, R. R. Schrock and A. H. Hoveyda, *J. Am. Chem. Soc.*, 2013, **135**, 6026–6029.

12 For ruthenium catalysts, see: (*a*) K. Endo and R. H. Grubbs, *J. Am. Chem. Soc.*, 2011, **133**, 8525–8527; (*b*) B. K. Keitz, K. Endo, P. R. Patel, M. B. Herbert and R. H. Grubbs, *J. Am. Chem. Soc.*, 2012, **134**, 693–699; (*c*) R. K. M. Khan, R. V. O'Brien, S. Torker, B. Li and A. H. Hoveyda, *J. Am. Chem. Soc.*, 2012, **134**, 12774–12779; (*d*) M. B. Herbert, V. M. Marx, R. L. Pederson and R. H. Grubbs, *Angew. Chem. Int. Ed.*, 2013, **52**, 310–314; (*e*) H. Miyazaki, M. B. Herbert, P. Liu, X. Dong, X. Xu, B. K. Keitz, T. Ung, G. Mkrtumyan, K. N. Houk and R. H. Grubbs, *J. Am. Chem. Soc.*, 2013, **135**, 5848–5858; (*f*) S. Torker, R. K. M. Khan and A. H. Hoveyda, *J. Am. Chem. Soc.*, 2014, **136**, 3439–3455; (*g*) J. S. Cannon, L. Zou, P. Liu, Y. Lan, D. J. O'Leary, K. N. Houk and R. H. Grubbs, *J. Am. Chem. Soc.*, 2014, **136**, 6733–6743.

13 (*a*) Y. Schrodi and R. L. Pederson, *Aldrichimica Acta*, 2007, **40**, 45–52; (*b*) S.-M. Paek, *Molecules*, 2012, **17**, 3348–3358.

14 T. W. Funk, J. M. Berlin and R. H. Grubbs, *J. Am. Chem. Soc.*, 2006, **128**, 1840–1846.

15 (*a*) J. M. Berlin, K. Campbell, T. Ritter, T. W. Funk, A. Chlenov and R. H. Grubbs, *Org. Lett.*, 2007, **9**, 1339–1342; (*b*) I. C. Stewart, T. Ung, A. A. Pletnev, J. M. Berlin, R. H. Grubbs and Y. Schrodi, *Org. Lett.*, 2007, **9**, 1589–1592; (*c*) I. C. Stewart, C. J. Douglas and R. H. Grubbs, *Org. Lett.*, 2008, **10**, 441–444.

16 C. K. Chung and R. H. Grubbs, *Org. Lett.*, 2008, **10**, 2693–2696.

17 (*a*) S. H. Hong, A. Chlenov, M. W. Day and R. H. Grubbs, *Angew. Chem. Int. Ed.*, 2007, **46**, 5148–5151; (*b*) K. Vehlow, S. Gessler and S. Blechert, *Angew. Chem. Int. Ed.*, 2007, **46**, 8082–8085.

18 (*a*) J. Mathew, N. Koga and C. H. Suresh, *Organometallics*, 2008, **27**, 4666–4670; (*b*) A. Poater and L. Cavallo, *J. Mol. Catal. A: Chem.*, 2010, **324**, 75–79; (*c*) A. Poater, N. Bahri-Laleh and L. Cavallo, *Chem. Commun.*, 2011, **47**, 6674–6676.

View Article Online
DOI: 10.1039/C5DT00453K
Journal Name



19 (*a*) F. Grisi, A. Mariconda, C. Costabile, V. Bertolasi and P. Longo, *Organometallics*, 2009, **28**, 4988–4995; (*b*) C. Costabile, A. Mariconda, L. Cavallo, P. Longo, V. Bertolasi, F. Ragone and F. Grisi, *Chem. Eur. J.*, 2011, **17**, 8618–8629.

20 Y. Borguet, G. Zaragoza, A. Demonceau and L. Delaude, *Dalton Trans.*, 2013, **42**, 7287–7296.

21 L. Benhamou, E. Chardon, G. Lavigne, S. Bellemin-Laponnaz and V. César, *Chem. Rev.*, 2011, **111**, 2705–2733.

22 Y. Borguet, G. Zaragoza, A. Demonceau and L. Delaude, *Adv. Synth. Catal.*, 2012, **354**, 1356–1362.

23 (*a*) F. M. Rivas, U. Riaz, A. Giessert, J. A. Smulik and S. T. Diver, *Org. Lett.*, 2001, **3**, 2673–2676; (*b*) F. M. Rivas, A. J. Giessert and S. T. Diver, *J. Org. Chem.*, 2002, **67**, 1708–1711.

24 For selected applications in the synthesis of *N*-alkyl and *N*-aryl benzimidazolium derivatives, see: (*a*) N. Hadei, E. A. B. Kantchev, C. J. O'Brien and M. G. Organ, *Org. Lett.*, 2005, **7**, 1991–1994; (*b*) D. M. Khramov, A. J. Boydston and C. W. Bielawski, *Org. Lett.*, 2006, **8**, 1831–1834; (*c*) A. R. Chianese, A. Mo and D. Datta, *Organometallics*, 2009, **28**, 465–472; A. R. Chianese, P. T. Bremer, C. Wong and R. J. Reynes, *Organometallics*, 2009, **28**, 5244–5252; (*d*) J. A. V. Er, A. G. Tennyson, J. W. Kamplain, V. M. Lynch and C. W. Bielawski, *Eur. J. Inorg. Chem.*, 2009, 1729–1738.

25 As a rule of the thumb, azolium tetrafluoroborates are often more easily handled and purified than the corresponding chlorides. For other illustrations of this principle, see: (*a*) A. Gómez-Suárez, R. S. Ramón, O. Songis, A. M. Z. Slawin, C. S. J. Cazin and S. P. Nolan, *Organometallics*, 2011, **30**, 5463–5470; (*b*) S. Meiries, K. Speck, D. B. Cordes, A. M. Z. Slawin and S. P. Nolan, *Organometallics*, 2012, **32**, 330–339.

26 (*a*) F. E. Hahn, L. Wittenbecher, R. Boese and D. Bläser, *Chem. Eur. J.*, 1999, **5**, 1931–1935; (*b*) F. E. Hahn, L. Wittenbecher, D. Le Van and R. Fröhlich, *Angew. Chem. Int. Ed.*, 2000, **39**, 541–544; (*c*) J. W. Kamplain and C. W. Bielawski, *Chem. Commun.*, 2006, 1727–1729; (*d*) D. M. Khramov, A. J. Boydston and C. W. Bielawski, *Angew. Chem. Int. Ed.*, 2006, **45**, 6186–6189.

27 R. W. Alder, M. E. Blake, L. Chaker, J. N. Harvey, F. Paolini and J. Schütz, *Angew. Chem. Int. Ed.*, 2004, **43**, 5896–5911.

28 D. Tapu, D. A. Dixon and C. Roe, *Chem. Rev.*, 2009, **109**, 3385–3407.

29 (*a*) H.-W. Wanzlick and E. Schikora, *Angew. Chem.*, 1960, **72**, 494; (*b*) H.-W. Wanzlick and E. Schikora, *Ber. Dtsch. Chem. Ges.*, 1961, **94**, 2389–2393; (*c*) V. P. W. Böhm and W. A. Herrmann, *Angew. Chem. Int. Ed.*, 2000, **39**, 4036–4038; (*d*) M.-J. Cheng, C.-L. Lai and C.-H. Hu, *Mol. Phys.*, 2004, **102**, 2617–2621; (*e*) M. K. Denk, A. Hezarkhani and F.-L. Zheng, *Eur. J. Inorg. Chem.*, 2007, 3527–3534.

30 (*a*) E. Çetinkaya, P. B. Hitchcock, H. Kücükbay, M. F. Lappert and S. Al-Juaid, *J. Organomet. Chem.*, 1994, **481**, 89–95; (*b*) J. W. Kamplain, V. M. Lynch and C. W. Bielawski, *Org. Lett.*, 2007, **9**, 5401–5404.

31 (*a*) R. Dorta, E. D. Stevens, N. M. Scott, C. Costabille, L. Cavallo, C. D. Hoff and S. P. Nolan, *J. Am. Chem. Soc.*, 2005, **127**, 2485–2495; (*b*) A. Fürstner, M. Alcarazo, H. Krause and C. W. Lehmann, *J. Am. Chem. Soc.*, 2007, **129**, 12676–12677; (*c*) S. Fantasia, J. L. Petersen, H. Jacobsen, L. Cavallo and S. P. Nolan, *Organometallics*, 2007, **26**, 5880–5889; (*d*) R. A. Kelly, III, H. Clavier, S. Giudice, N. M. Scott, E. D. Stevens, J. Bordner, I. Samardjiev, C. D. Hoff, L. Cavallo and S. P. Nolan, *Organometallics*, 2008, **27**, 202–210; (*e*) L. Delaude, A. Demonceau and J. Wouters, *Eur. J. Inorg. Chem.*, 2009, 1882–1891; (*f*) S. Wolf and H. Plenio, *J. Organomet. Chem.*, 2009, **694**, 1487–1492.

32 R. Savka and H. Plenio, *Dalton Trans.*, 2015, **44**, 891–893.

33 M. Iglesias, D. J. Beetstra, B. Kariuki, K. J. Cavell, A. Dervisi and I. A. Fallis, *Eur. J. Inorg. Chem.*, 2009, 1913–1919.

34 (*a*) P. A. Evans, E. W. Baum, A. N. Fazal and M. Pink, *Chem. Commun.*, 2005, 63–65; (*b*) W. A. Herrmann, J. Schütz, G. D. Frey and E. Herdtweck, *Organometallics*, 2006, **25**, 2437–2448; (*c*) S. Burling, M. F. Mahon, S. P. Reade and M. K. Whittlesey, *Organometallics*, 2006, **25**, 3761–3767; (*d*) D. M. Khramov, V. M. Lynch and C. W. Bialewski, *Organometallics*, 2007, **26**, 6042–6049; (*e*) A. P. Blum, T. Ritter and R. H. Grubbs, *Organometallics*, 2007, **26**, 2122–2124; (*f*) A. Bittermann, P. Härter, E. Herdtweck, S. D. Hoffmann and W. A. Herrmann, *J. Organomet. Chem.*, 2008, **693**, 2079–2090.

35 F. Ragone, A. Poater and L. Cavallo, *J. Am. Chem. Soc.*, 2010, **132**, 4249–4258.

36 (*a*) A. C. Hillier, W. J. Sommer, B. S. Yong, J. L. Petersen, L. Cavallo and S. P. Nolan, *Organometallics*, 2003, **22**, 4322–4326; (*b*) L. Cavallo, A. Correa, C. Costabille and H. Jacobsen, *J. Organomet. Chem.*, 2005, **690**, 5407–5413; (*c*) S. Díez-González and S. P. Nolan, *Coord. Chem. Rev.*, 2007, **251**, 874–883; (*d*) H. Clavier and S. P. Nolan, *Chem. Commun.*, 2010, **46**, 841–861.

37 A. Poater, B. Cosenza, A. Correa, S. Giudice, F. Ragone, V. Scarano and L. Cavallo, *Eur. J. Inorg. Chem.*, 2009, 1759–1766.

38 A. Poater, F. Ragone, R. Mariz, R. Dorta and L. Cavallo, *Chem. Eur. J.*, 2010, **16**, 14348–14353.

39 TEP ($cm^{-1}$) = 0.8001 $\nu_{CO}^{Rh,average}$ + 420, see: T. Dröge and F. Glorius, *Angew. Chem. Int. Ed.*, 2010, **49**, 6940–6952.

40 (*a*) M. Süßner and H. Plenio, *Chem. Commun.*, 2005, 5417–5419; (*b*) J. P. Moerdyk and C. W. Bielawski, *Organometallics*, 2011, **30**, 2278–2284; (*c*) G. A. Blake, J. P. Moerdyk and C. W. Bielawski, *Organometallics*, 2012, **31**, 3373–3378.

41 For other uses of this phosphine scavenger in the synthesis of ruthenium-isopropoxyalkylidene complexes, see: (*a*) H. Wakamatsu and S. Blechert, *Angew. Chem. Int. Ed.*, 2002, **41**, 794–796; (*b*) S. J. Connon, M. Rivard, M. Zaja and S. Blechert, *Adv. Synth. Catal.*, 2003, **345**, 572–575; (*c*) N. Buschmann, H. Wakamatsu and S. Blechert, *Synlett*, 2004, 667–670; (*d*) K. Vehlow, S. Maechling and S. Blechert, *Organometallics*, 2006, **25**, 25–28; (*e*) K. Grela, S. Harutyunyan and A. Michrowska, *Angew. Chem. Int. Ed.*, 2002, **41**, 4038–4040; (*f*) A. Michrowska, S. Harutyunyan, V. Sashuk, G. Dolgonos and K. Grela, *J. Am. Chem. Soc.*, 2004, **126**, 9318–9325; (*g*) M. Bieniek, A. Michrowska, Ł. Gułajski and K. Grela, *Organometallics*, 2007, **26**, 1096–1099; (*h*) D. Rix, F. Caijo, I. Laurent, F. Boeda, H. Clavier, S. P. Nolan and M. Mauduit, *J. Org. Chem.*, 2008, **73**, 4225–4228.

42 (*a*) A. Fürstner, L. Ackermann, B. Gabor, R. Goddard, C. W. Lehmann, R. Mynott, F. Stelzer and O. R. Thiel, *Chem. Eur. J.*, 2001, **7**, 3236–3253; (*b*) G. C. Vougioukalakis and R. H. Grubbs, *Organometallics*, 2007, **26**, 2469–2472; (*c*) M. M. Gallagher, A. D. Rooney and J. J. Rooney, *J. Organomet. Chem.*, 2008, **693**, 1252–1260; (*d*) S. Leuthäusser, V. Schmidts, C. M. Thiele and H. Plenio,

View Article Online
DOI: 10.1039/C5DT00455K ARTICLE

*Chem. Eur. J.*, 2008, **14**, 5465–5481; (*e*) A. Perfetto, C. Costabile, P. Longo and F. Grisi, *Organometallics*, 2014, **33**, 2747–2759.

43 (*a*) K. Weigl, K. Köhler, S. Dechert and F. Meyer, *Organometallics*, 2005, **24**, 4049–4056; (*b*) M. Barbasiewicz, A. Szadkowska, A. Makal, K. Jarzembska, K. Woźniak and K. Grela, *Chem. Eur. J.*, 2008, **14**, 9330–9337; (*c*) K. M. Kuhn, J.-B. Bourg, C. K. Chung, S. C. Virgil and R. H. Grubbs, *J. Am. Chem. Soc.*, 2009, **131**, 5313–5320; (*d*) I. C. Stewart, D. Benitez, D. J. O'Leary, E. Tkatchouk, M. W. Day, W. A. Goddard, III and R. H. Grubbs, *J. Am. Chem. Soc.*, 2009, **131**, 1931–1938; (*e*) S. Tiede, A. Berger, D. Schlesiger, D. Rost, A. Lühl and S. Blechert, *Angew. Chem. Int. Ed.*, 2010, **49**, 3972–3975; (*f*) A. Perfetto, C. Costabile, P. Longo, V. Bertolasi and F. Grisi, *Chem. Eur. J.*, 2013, **19**, 10492–10496.

44 M. Barbasiewicz, M. Bieniek, A. Michrowska, A. Szadkowska, A. Makal, K. Wozniak and K. Grela, *Adv. Synth. Catal.*, 2007, **349**, 193–203.

45 T. Ritter, A. Hejl, A. G. Wenzel, T. W. Funk and R. H. Grubbs, *Organometallics*, 2006, **25**, 5740–5745.

46 M. Bieniek, A. Michrowska, D. L. Usanov and K. Grela, *Chem. Eur. J.*, 2008, **14**, 806–818.

View Article Online
DOI: 10.1039/C5DT00433K

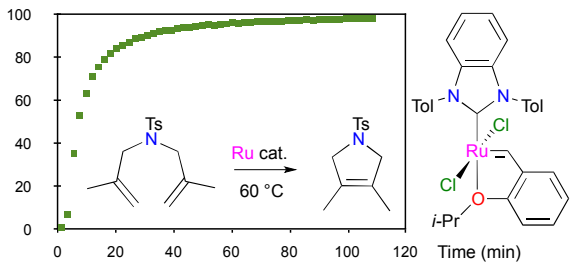


Second-generation ruthenium–alkylidene complexes featuring the 1,3-di(2-tolyl)imidazol-2-ylidene ligand (BTol) are highly efficient catalysts for the synthesis of tetrasubstituted cycloolefins via ring-closing metathesis (RCM).